Available online at www.sciencedirect.com
SCIENCE DIRECT
Thin Solid Films 501 (2006) 291 – 294
thin solid films
www.elsevier.com/locate/tsf

A combined experimental and computer simulation study of HWCVD nip microcrystalline silicon solar cells

J.J.H. Strengers [b], F.A. Rubinelli [a,*], J.K. Rath [b], R.E.I. Schropp [b]

[a] INTEC, Universidad Nacional del Litoral, Güemes 3450, 3000, Santa Fe, Argentina
[b] Utrecht University, Debye Institute, SID — Physics of Devices, P.O. Box 80000, 3508 TA Utrecht, The Netherlands

Available online 15 August 2005

Abstract

Microcrystalline silicon solar cells with intrinsic layer thicknesses between 500 and 3000 nm deposited using the hot-wire CVD technique are investigated, combining experimental characterisation with computer simulations. Fitting of the solar cell characteristic curves shows that this material has a density of dangling bonds and drift mobility that are comparable to that of amorphous silicon, whereas its mobility band gap is closer to the value of crystalline silicon. These fittings can be done assuming homogeneous electrical parameters in the intrinsic layers. A maximum in solar cell performance was seen for i-layer thickness of 3000 nm.

Keywords: Solar cells; Hot-wire deposition; Microcrystalline silicon

1. Introduction

Microcrystalline silicon (μc-Si) is a two-phase material in which crystalline regions are embedded in an amorphous matrix. This type of silicon has received great attention over the last years because of its better optical absorption than crystalline silicon. Also, unlike amorphous silicon, it has stable transport properties that are not influenced by light induced degradation. It is known that the grain boundaries are important parts of the microstructure of μc-Si. There are two kinds of crystalline grains, small (SG) and large grains (LG) [1].

In this paper we combine experimental characterization with computer simulations in order to gain a better insight of the transport mechanisms controlling the solar cell performance of single-junction nip μc-Si structures where the intrinsic layer has been deposited by the hot-wire CVD technique. For the simulations, we used the computer program D-AMPS developed at Penn State University (USA) and INTEC (Argentina) [2]. From previous research [3] we expected the crystalline regions to be homogeneously distributed over the i-layer that is deposited at a silane/hydrogen ratio of 5:100. We investigated this prediction with computer simulations. Solar cells with different i-layer thicknesses were deposited in order to determine the optimal i-layer thickness for this type of material and cells.

2. Experimental

Solar cells in n-i-p configuration have been grown on plain stainless steel substrates (no optical enhanced back reflector), by growing HWCVD intrinsic layers covering a wide range of thicknesses (500–3000 nm) and using ITO as top contact. The crystalline ratio (ratio of the intensities of crystalline and amorphous fraction of the transverse-optical Si–Si vibration of the Raman spectrum) of the HW μc-Si layers used in the cells was found to vary slightly in the range of 44%–47%. The optical absorption in the red region is much higher in HW μc-Si than in amorphous silicon. The doped layers of the cell were deposited with the PECVD technique. Solar cells were characterized by measuring dark and light current voltage (J–V) characteristics and spectral response (SR) curves without bias light and with bias light at 0 and −2 V.

* Corresponding author.
E-mail address: pancho@ceride.gov.ar (F.A. Rubinelli).

0040-6090/$ - see front matter © 2005 Elsevier B.V. All rights reserved.
doi:10.1016/j.tsf.2005.07.198

3. Results

Dark $J-V$ curves show saturation at forward voltages beginning at 0.6 V and also show consistency with i-layer thickness. The open circuit voltages of these cells are comparable and around 0.5 V. SR measurements made without bias light and with bias light at 0 and −2 V do not show any significant differences, indicating that light trapping effects are not limiting the solar cell short circuit current. Moreover, SR curves do not show a significant improvement of the red response for i-layers thicker than 2 μm.

3.1. Fitting dark $J-V$ and light $J-V$ experiments

Fig. 1 shows the dark $J-V$ experimental curves together with the simulated fit for cells with i-layer thickness of 1000 nm and 3000 nm. Only the fits of the samples with the thinnest and thickest i-layers are included to keep the figure clear. A similar fit of the dark $J-V$ curve are obtained for the solar cell with i-layer thicknesses of 2000 nm. Fig. 2 shows the light $J-V$ experimental curves together with the simulated fits for cells with i-layer thicknesses of 1000, 2000 and 3000 nm. The cell of 500 nm i-layers showed considerable shunting to be properly fitted without including in our modelling the presence of an extra shunt resistance. The dark $J-V$ was considered to be fitted once the simulated and the experimental curves at forward voltages visually overlapped. The current at reverse voltage could not be fitted for all i-layers thicknesses because the experimental current at reverse voltage is nearly equal for different thicknesses whereas simulations always show higher reverse current for thicker i-layers. The light $J-V$ was considered to be fitted once the deviations of the most essential simulated output parameters (J_{sc}, V_{oc} and FF) were within a range of 7.5% of the experimental values except for the FF of the 2000 nm cell due to some minor shunting behaviour. Although not shown in Fig. 2, the light $J-V$ curve was also successfully matched for reverse voltages.

Our simulations were first run relying on input parameters coming from PECVD μc-Si p-i-n-layers used in a previous simulation research [4] performed on n-i-p μc-Si tunnel recombination junctions (TRJ) in a-Si/a-Si tandem solar cells. Changes of electrical parameters inside the i-μc-layer were made accordingly only in order to match the experimental curves. The fitted simulations for the dark $J-V$ turned out to be sensitive at low forward voltages and reverse voltages only for changes of the dangling bond e^-/h^+ capture cross section and densities. This indicates that the dark current for low forward voltages is controlled by recombination through the mid-gap states and that the dark current at reverse voltages is controlled by thermal generation of electron-hole pairs from mid-gap states. The saturation of the current visible in Fig. 1 for higher voltages (>0.6 V) could be reproduced in our simulations by imposing a limitation to hole injection at the front contact by the presence of band bending.

In Table 1, the most essential electrical parameters values of the intrinsic material used as inputs to fit the experimental curves are shown. These parameters resulted to be the same for the three different thicknesses except for the capture cross sections (donor- and acceptor-like states), which were a factor 3 lower for the sample with 3000 nm i-layer thickness. In our simulations changes in the input values were made only for the i-layer since just this layer has been deposited with the HWCVD technique. We have to keep in mind that the high values of mobilities used in our simulations (see Table 1) are extended state mobilities (μ_E). The measured mobilities

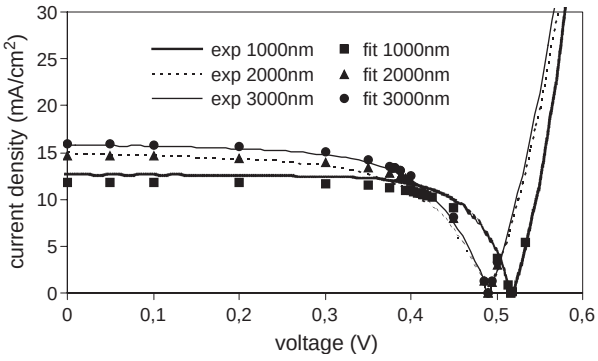

Fig. 2. The fitted light $J-V$ curves for 1000, 2000 and 3000 nm i-layer thicknesses.

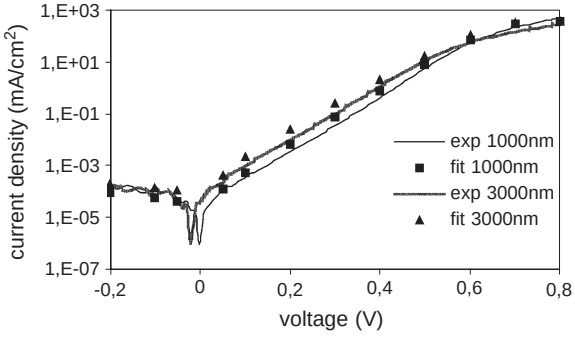

Fig. 1. The fitted dark $J-V$ curves for 1000 nm i-layer thicknesses.

Table 1
Essential input parameters adopted in the i-layer

Input parameter	Value
Global density of dangling bonds (donor- and acceptor-like states) (cm^{-3})	2.5×10^{15}
Effective density of states N_c, N_v (cm^{-3})	3×10^{19}
Electron/hole extended state mobility ($cm^2/V-s$)	150/75
Cross-section in donor-like states: charged/neutral (cm^2)	$2.5\times10^{-14}/2.5\times10^{-15}$
Cross section in acceptor-like states: neutral/charged (cm^2)	$2.5\times10^{-15}/2.5\times10^{-14}$
Mobility band gap (eV)	1.25

are much lower because they really are drift mobilities (μ_D). For electrons they are related by the equation $\mu_D=\mu_E*n/(n+n_t)$ where n is the free electron concentration and n_t the trapped electron concentration. A similar equation can be written for holes. The ratio $n/(n+n_t)$ is around 1:400 calculated at $V=0$ and under 1.5 AM illumination at the i-layer bulk. Microcrystalline Si is a two-phase material: (amorphous and crystalline) with both materials having a different mobility band gaps (~1.76 eV and 1.12 eV, respectively). The μc-Si band gap used in our simulations should be interpreted as an 'effective mobility band gap'. There is some discrepancy in the literature about its actual value that is usually adopted between 1.2 eV and 1.6 eV [5].

We also intended to fit the experimental curves by grading some essential electrical input parameters linearly within the intrinsic layer. By doing this, we presumed the intrinsic layer to be inhomogeneous. However the simulated open circuit voltage and current increased in comparison to the non-graded simulation, thus the graded simulation did not fit the experimental curves as well as the non-graded simulation.

3.2. Fitting spectral response experiments

Fig. 3 shows experimental spectral response curves measured under AM 1.5 bias light together with their fits for i-layer thicknesses of 1000, 2000 and 3000 nm. The simulations showed the same trends observed in the experiments, giving as output the same curves for the spectral response with and without bias light and/ or −2 V, indicating that light trapping effects do not affect the solar cell short circuit current.

Our initial simulated response for wavelengths between 600 and 750 nm resulted in too low values in comparison to the experimental response. Therefore we presumed a slight scattering of light with a cosθ angular distribution at the i-n layer interface. An increase in response means an increase in short circuit current. However, this increase was rather small in comparison with the change in short circuit current caused by changes in optical band gap and mobilities.

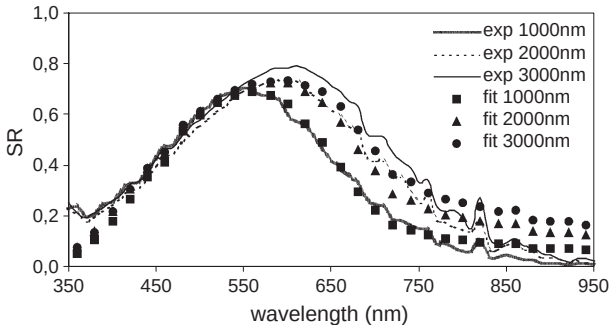

Fig. 3. The fitted short-circuit spectral response curves under bias light for 1000, 2000 and 3000 nm i-layer thickness.

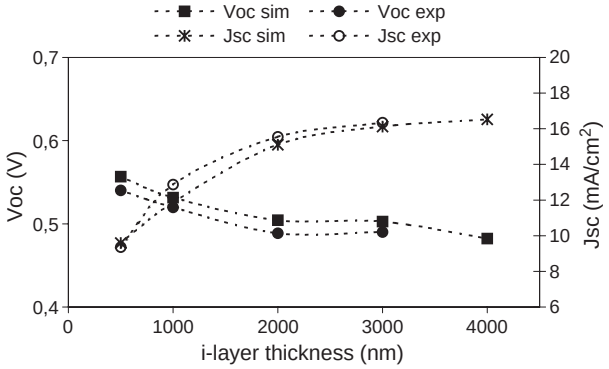

Fig. 4. Experimental and simulated V_{oc} and J_{sc} for different i-layer thicknesses.

3.3. Comparison of light J–V outputs for different i-layer thicknesses

In solar cells a high series resistance would lower the fill factor (FF) and the short circuit current (J_{sc}) but would not affect the open circuit voltage (V_{oc}). A low shunting resistance would lower the fill factor and the V_{oc}, but would leave the J_{sc} unaffected [6]. However the influence on the J_{sc} and V_{oc} is small as long as the series resistance is not much higher than 10 Ω cm^2 and the shunting resistance is not lower than 100 Ω cm^2. This is the case for the sample with an i-layer thickness of 500 nm and therefore it is possible to simulate V_{oc} and J_{sc} for this sample without taking into account possible shunts.

In Fig. 4 the experimental and simulated V_{oc} and J_{sc} are compared for i-layer thicknesses of 500, 1000, 2000 and 3000 nm. To get an idea of the performance of a cell with 4000 nm i-layer thickness, we ran a simulation using the same input parameters as for the other simulations. The deviation of the experimental and simulated values for the V_{oc} in percentage ranges between 2.3% (1000 nm) and 3.2% (2000 nm). For the J_{sc} the deviation is between 1.3% (3000 nm) and 7.5% (1000 nm). Fig. 4 shows that the simulated values of the V_{oc}/J_{sc} follow the same trend as the

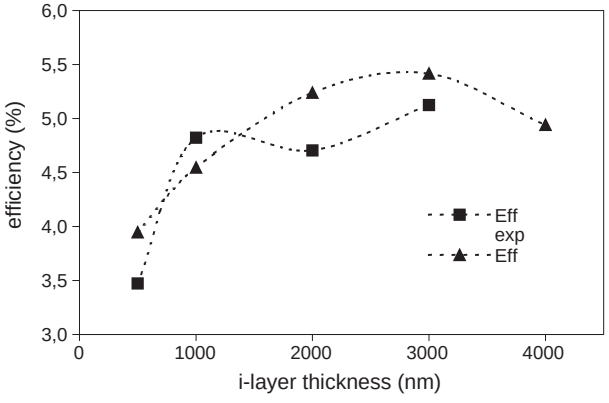

Fig. 5. Experimental and simulated efficiencies for different i-layer thicknesses.

experimental values: both decrease/increase for an increase in the i-layer thickness from 500 nm to 1000 nm and remain quite constant for an i-layer thickness in the range of 2000–4000 nm. This effect was also visible when we compared the experimental and simulated spectral response (with and without light bias) for the different i-layer thicknesses. The red response significantly increased as the i-layer thickness increases up to 2000 nm. The result of this can be seen in Fig. 5: keeping in mind that the cells with i-layer thickness of 500 and 2000 nm show (minor) shunting behaviour, the experimental efficiencies for the different thicknesses follow the same trend as the simulated values. Combining this with the predicted value for a cell with a 4000 nm i-layer, a maximum is observed for an i-layer thickness of 3000 nm.

4. Conclusions

The experimental characterization $J-V$ and SR curves of a series of HWCVD n-i-p solar cells could be fitted within an acceptable range (<7.5%) for different intrinsic layer thicknesses. These fittings provide us with information on the transport mechanisms controlling the performance of these solar cells. Single-junction μc-Si nip cells with intrinsic layer deposited by hot-wire CVD technique turned out to have a density of dangling bonds and drift mobility comparable to amorphous silicon, but with a lower mobility band gap. The solar cell characteristic curves were successfully fitted assuming homogeneous intrinsic layers with very minor differences in the electrical parameters for different thicknesses and unsuccessfully fitted assuming a non-homogeneous intrinsic layer. This indicates that this material has a homogeneous distribution of the crystalline grains (SG and LG) in the amorphous matrix. When we compare the experimental and the simulated characteristic curves $J-V$ and SR for different intrinsic layer thicknesses we observe the optimal intrinsic layer thickness to be around 3000 nm.

Acknowledgments

We would like to thank Karine van der Werf for deposition of the samples used for this research. We appreciate the financial support from Utrecht University and Agencia Nacional de Promoción Científica y Tecnológica.

References

[1] J. Koka, et al., Sol. Energy Mater. Sol. Cells 78 (1–4) (2003) 493.
[2] E. Klimovsky, et al., J. Non-Cryst. Solids 338–340 (2004) 686.
[3] M. van Veen, Tandem Solar Cells deposited using Hot-Wire Chemical Vapor Deposition, PhD thesis, Utrecht University (2003).
[4] J.K. Rath, F.A. Rubinelli, R.E.I. Schropp, J. Non-Cryst. Solids 266–269 (2000) 1129.
[5] N. Palit, P. Chaterjee, J. Appl. Phys. 86 (1999) 6879.
[6] H.J. Hovel, Semiconductors and Semimetals, Academic Press, 1975, p. 62.